

EFFECT OF THE PAULI PRINCIPLE IN O^{16} - O^{16} ELASTIC SCATTERING

Barry Block*

Physics Department and the Institute of Geophysics and Physics,
The University of California, San Diego, La Jolla, California

and

F. B. Malik†

Physics Department, Yale University, New Haven, Connecticut

(Received 16 June 1967)

The 90° differential scattering cross section for the O^{16} - O^{16} elastic scattering seen by Siemsen *et al.*¹ shows striking regularities in the energy region 17 to 35 MeV in the c.m. system. The cross section shows the usual Coulomb scattering form at lower energies, but in the 17- to 35-MeV region there are three very-well-defined peaks, each with a width about 2 MeV. These peaks are spaced at about 4-5 MeV, with the peak spacing increasing slowly with energy. The ratio of peak-to-valley cross sections is about 10 to 1. The peak cross sections are roughly equal and each peak is broken into three smaller peaks which themselves are evenly spaced.

The existence of such a regular series of features in the scattering of two complicated nuclei behooves one to look for a simple explanation. Since the energy region involved is not far removed from the Coulomb barrier, the effect of the barrier is expected to come into any description of this process. Surmounting this barrier forms the first step in the interaction process. At this point there are two competing effects: the nuclear potential and the Pauli principle. Although the nuclei are within the range of each other's nuclear well, the net result of this elastic process is the coherent scattering of 16 particles on 16 particles. This coherence is mirrored by the fact that the entrance and the exit channels are identical, and it is caused by the Pauli principle which overcomes the coherence-destroying effects of the attractive internucleon potential.

With this idea in mind, the second step of the interaction process is determined by a nuclear potential dominated by the Pauli principle. Such a potential could have, as a function of internuclear distance r , the form of a repulsive core with an attractive well at a larger radius (Fig. 1). There is an analogy between this nuclear potential and the intermolecular potential represented by the Lennard-Jones model.² The effective potential is then the sum

of the Pauli-principle-dominated nuclear potential and a potential barrier which is a sum of the Coulomb and the centrifugal barriers at the nuclear surface.

The sum could have the form shown in Fig. 1 with a dip between the repulsive core and the top of an effective barrier. The bottom of the effective well can even be above zero energy. The height of the well and the effective well size are determined by the competition between the effective barrier (which is, in principle, a sum of the Coulomb and angular-momentum barriers) and the Pauli-principle-dominated nuclear field. One can see with such a picture that virtual states of the system can occur for system energies above the effective barrier leading to resonant features in the cross section. A similar phenomenon exists in the case of molecular scattering when a similar potential configuration is formed with a Lennard-Jones potential and the centrifugal barrier potential.³ A series of virtual scattering states exists and phenomena associated with these states would be found in the cross section. The general features associated with such a model would be slowly varying functions of A and Z .

To apply these ideas for an initial orientation to the phenomena seen in the (O^{16} - O^{16}) elastic scattering, one can make a one-dimensional model of such a potential, calculate the transmission coefficient and the cross section, and investigate whether a reasonable choice of pa-

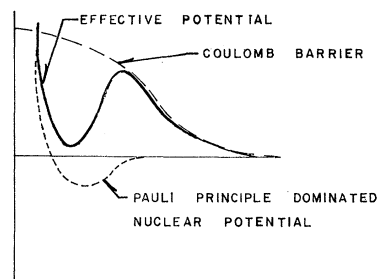


FIG. 1. Effective potential well.

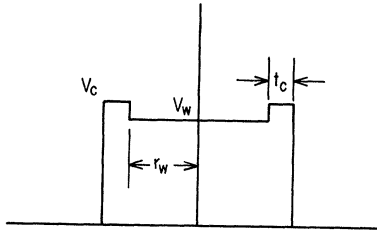


FIG. 2. The schematic potential used in this model. The abscissa and ordinates represent, respectively, the range and depth of the potential.

rameters leads to a description of these phenomena and gives, even in this very simple approximation, the dependence of these phenomena on energy and potential parameters.

The extreme one-dimensional potential chosen was a square-well model (Fig. 2) with an effective barrier V_c , barrier thickness t_c , and a well depth (now positive energy) V_w with range r_w . The transmission coefficient of such a potential in the JWKB approximation⁴ is

$$T = [1 + \frac{1}{4}(4\theta^2 - 1/4\theta^2)^2 \sin^2 \frac{1}{2}(\pi - J/\hbar)]^{-1},$$

where the penetrability is

$$\theta = \exp \frac{1}{\hbar} \int_{\text{range}}^{\text{Coulomb}} p_c dx$$

and the phase integral,

$$J = 2 \int_{\text{range}}^{\text{Nuclear}} p_w dx.$$

p_c and p_w are, respectively, the momenta inside the effective barrier and effective well and are, respectively, $[2\mu(E - V_c)]^{1/2}$ and $[2\mu(E - V_w)]^{1/2}$ in this simple model. Such a trans-

mission factor will give cross-section maxima ($T = 1$) when

$$\pi - J/\hbar = -2N\pi \text{ or } J_n = (2N+1)\pi\hbar.$$

The cross section σ in this simple model is given by T/E . It is interesting that the condition for the "resonance" is exactly the same as that for a bound state. An important feature of the potential of Fig. 2 is that in comparison with an attractive well without barriers, the penetrability associated with this model is considerably larger, giving large peak-to-valley ratios.

The experimental data, at 90° in the c.m. system, smoothed with a running five-point mean over 1 MeV to average out the small peaks and obtain the gross structure, is used to obtain quantities of interest. Table I contains experimentally determined peak energies, peak spacings, widths, and peak-to-valley cross-section ratios. Widths listed here are determined from the energies at which the cross section falls to one-half of its maximum value.

It should be noted that there is a partially buried peak at about 17.5 MeV and a pair of small peaks at 32 and 35 MeV which have a much smaller peak-to-valley ratio than the others.

The parameters chosen for the square-well model are

$$V_c = 17.5 \text{ MeV},$$

$$t_c = 0.1 \text{ F},$$

$$V_w = 16.0 \text{ MeV},$$

$$r_w = 1.2A^{1/3} = 3 \text{ F}.$$

Table I. Comparison between the observed features (expt) and the theory (calc). (Energy, width in MeV.)

Resonance energy		Peak-to-valley ratio		Valley energy		Resonance half-width		Valley width	
Expt	Calc	Expt	Calc ^a	Expt	Calc	Expt	Calc	Expt	Calc
17.5	17.6	10	6	18.8	18.9			0.7	0.7
20.6	20.4	10	7.4	22.5	22.4	2.2	1.0	1.2	1.5
24.6	24.6	10	9.2	26.8	27.4	2.2	1.3	2.2	3
29.6	30.3	10	11.2	31.0	33.5	1.8	1.4		

^aIf t is changed to 0.2, the computed peak-to-valley ratios increase by about 80%, whereas the resonance half-width narrows only by about 10%.

The height of effective barrier V_c and the width of the well $2r_w$ are consistent with the estimate of the sum of centrifugal and Coulomb barriers on the nuclear surface and nuclear radius, respectively. Since the path of integration in θ involves the width of the barrier near its top, t_c is expected to be small. The depth of the well V_w , in the context of the model, reflects the magnitude of the Pauli-principle-dominated nuclear potential relative to the height of the effective barrier. It is this difference that produces the cross-section maxima. Quantities calculated, using the above choice of parameters, are found in Table I.

The interesting feature of this model is that with the choice of two, so-far-arbitrary numbers V_w and t_c , and with reasonable choices for two other parameters, one can reproduce (see Table I) (i) the experimental locations of a whole series of peaks, (ii) the valley locations, (iii) the peak widths, and (iv) the peak-to-valley ratios. The model furthermore predicts that (i) at the valleys cross sections are very small, and (ii) that the valley is flat as observed and the width of the valley increases with the energy, e.g., the valley between the peaks at 29.6 and 24.6 should be larger than the width of the previous valley. These features agree with the experiment. In short, the theoretical excitation function reproduces the experimental curve up to 31 MeV. Beyond that energy the theory does not predict further large peaks, e.g., the next peak around 37 MeV should only be half the size of the 20.6-MeV peak. Thus in this schematic model the cross section beyond 31 MeV essentially falls off slowly as $1/E$, which agrees with the experiment.

It has already been felt⁴⁻⁸ that the analysis of the elastic scattering data involving heavy ions, e.g. (C^{12}, C^{12}) may require a shallow potential.

The apparent success of this schematic model leads to the hypothesis that a model which would give angular distributions and other features can be concocted using a Lennard-Jones potential with an appropriate Coulomb and centrifugal barrier. The main point of the present Letter is to indicate that such a sophisticated treatment should incorporate a very shallow potential, preferably of Lennard-Jones type with a hard or soft core. These results also encourage one to seek a deeper explanation for the nature of V_w in terms of a theory of either the Bethe-Goldstone or the resonating

group⁹ type. Such a treatment would surely lead to a strong velocity-dependent potential arising from particle exchange (nucleons, alphas, etc.) between the two oxygen nuclei, very much in the same way that one gets a strong velocity-dependent interaction between two alpha particles due to the nucleonic exchange¹⁰ (or the repulsive core of the two nucleon potential arising from pion exchange¹¹). This velocity-dependent potential can then be approximated with an energy-dependent repulsive core followed at large radii by a shallow smooth attractive potential.

The transmission maxima of Table I can be assumed to couple to various impurities such as small intrinsic vibrational states of each O^{16} (or other intrinsic states, such as multi-particle-hole states). This coupling results (i) in generating a fine structure on each peak (for a linear coupling they should be uniformly spaced in energy) and (ii) in broadening the widths of each peak.¹²

As a final point, the question of where to look for other such phenomena can be examined with this model. They should not appear in the lightest nuclei since the Coulomb barrier is not high enough to create an effective well. For heavy nuclei, the Coulomb barrier is expected to increase faster than the repulsive Pauli exchange forces, giving rise to a deepening well. This will result in cross-section maxima whose width and spacing increase with nucleon number.

We thank Professor Bromley, Professor Siemssen, and Mr. Maher and Mr. Weidinger for discussions concerning the experimental results. We appreciate very much the illuminating discussion on this physical process with Professor H. Feshbach and Professor E. Mason. We furthermore thank Mr. P. Wasielewski for helping with the computation.

*Work supported in part by the National Science Foundation.

†Work supported in part by U. S. Atomic Energy Commission.

¹R. H. Siemssen, J. Maher, A. Weidinger, and D. A. Bromley, *Bull. Am. Phys. Soc.* **11**, 571 (1967); and to be published.

²R. J. Munn, E. A. Mason, and F. J. Smith, *J. Chem. Phys.* **41**, 3978 (1964).

³D. Bohm, *Quantum Theory* (Prentice Hall, Inc., New York, 1951).

⁴E. W. Vogt and H. McManus, *Phys. Rev. Letters* **4**, 518 (1960).

⁵R. H. Davis, Phys. Rev. Letters 4, 521 (1960).
⁶D. A. Bromley, J. A. Kuehner, and E. Almquist, Phys. Rev. 123, 878 (1961); E. Almquist, D. A. Bromley, J. A. Kuehner, and B. Whalen, Phys. Rev. 130, 1140 (1963).
⁷A. S. Kompaneets, Zh. Eksp. i Teor. Fiz. 39, 1713 (1960) [translation: Soviet Phys.-JETP 12, 1196 (1961)].

⁸K. Wildermuth and R. L. Carovillano, Nucl. Phys. 28, 636 (1961).
⁹J. A. Wheeler, Phys. Rev. 52, 1123 (1937).
¹⁰A. Herzenberg, Nucl. Phys. 3, 1 (1957); A. Herzenberg and A. S. Roberts, Nucl. Phys. 3, 314 (1957).
¹¹S. Gartenhaus, Phys. Rev. 100, 900 (1955).
¹²C. B. Duke, F. W. K. Firk, and F. B. Malik, Phys. Rev. 157 (1967).

ELASTIC ELECTRON SCATTERING FROM LEAD-208 AT 175 AND 250 MeV

J. B. Bellicard* and K. J. van Oostrum†

High Energy Physics Laboratory, Stanford University, Stanford, California

(Received 22 June 1967)

We have measured absolute cross sections for the elastic scattering of 175- and 250-MeV electrons from lead-208, and have carried out a partial-wave analysis of the data for a Fermi-type nuclear charge distribution described with two or three parameters. A comparison with low energy electron and muonic x-ray results is given.

High values of the incident electron energy or high values of the momentum transfer enable fine details to be revealed in the description of the static charge distribution of the nucleus.¹ On the other hand, x rays from muonic atoms lead to a precise measurement of the rms nuclear size.² It is interesting to know to what extent the two experiments complement each other in determining the nuclear charge distribution. Lead-208 is a spherical doubly magic nucleus and is specially useful for this investigation. We have carried out an experiment with 150- and 250-MeV electrons which covers a large field of momentum transfer. Experimental and computational procedures are similar to those of Hofstadter et al.³ The electron beam was supplied by the Stanford Mark-III linear accelerator. The target was an isotopically enriched foil of lead-208. The over-all energy resolution was 0.2%. The lowest ²⁰⁸Pb level is at 2.60 MeV and is well resolved from the elastic peak.

The differential elastic-scattering cross-section values have been measured in absolute units by comparing the data with the scattering cross sections from hydrogen contained in a comparison polyethylene (CH₂) target. The hydrogen cross sections were taken from well-established values at the same momentum-transfer conditions of this experiment. These cross sections have been corrected for finite aperture of the spectrometer and for angular spread of the incident electron beam.

In Tables I and II, we give the values of the

Table I. Elastic electron scattering cross sections on lead-208. Incident energy = 175 ± 1.0 MeV.

θ (deg)	Cross section (cm ² /sr)
32	$(1.883 \pm 0.088) \times 10^{-26}$
34	$(1.081 \pm 0.056) \times 10^{-26}$
36	$(6.371 \pm 0.300) \times 10^{-27}$
38	$(3.909 \pm 0.180) \times 10^{-27}$
40	$(2.615 \pm 0.105) \times 10^{-27}$
45	$(1.169 \pm 0.039) \times 10^{-27}$
49	$(6.471 \pm 0.233) \times 10^{-28}$
53	$(3.566 \pm 0.157) \times 10^{-28}$
58	$(1.443 \pm 0.076) \times 10^{-28}$
64	$(3.991 \pm 0.300) \times 10^{-29}$
69	$(1.347 \pm 0.106) \times 10^{-29}$
74	$(6.254 \pm 0.220) \times 10^{-30}$
80	$(4.228 \pm 0.117) \times 10^{-30}$
86	$(2.791 \pm 0.125) \times 10^{-30}$

cross sections for both experiments. Error bars include the statistical error and the uncertainties in energy (0.6%) and in angle (0.1°).

The interpretation of the above results has been carried out with the phase-shift method of calculation of the scattering process. The computational procedures are described elsewhere.⁴ An examination of the results has been made by using systematically a Fermi shape with two or three parameters:

$$\rho(r) = \rho_0 [1 + W_r^2/c^2] \{ \exp[(r-c)/z] + 1 \}^{-1},$$

where $z = t/4.4$. If $W = 0$, the parameter t corresponds to the 90-10% skin thickness.